Korean J. Chem. Eng., 32(10), 2031-2046 (2015)
DOI: 10.1007/s11814-015-0036-8

pISSN: 0256-1115
eISSN: 1975-7220

Sorption and desorption of hexavalent chromium using a novel brown marine algae *Sargassum myriocystum*

Rajagopal Jayakumar†, Manivasagan Rajasimman, and Chinnappan Karthikeyan

Environmental Engineering Laboratory, Department of Chemical Engineering, Annamalai University, Annamalainagar - 608002, Tamilnadu, India
(*Received 1 August 2014 • accepted 9 February 2015*)

Abstract−The present investigation deals with the sorption of Cr(VI) onto a marine brown algae *Sargassum myriocystum* in batch reactors. Response surface methodology (RSM) was used for the optimization of variables like pH, sorbent dosage (g/L), agitation speed (rpm) and contact time (min). A maximum percentage removal of Cr(VI) by *Sargassum myriocystum* occurs at the following conditions: pH - 5.2; sorbent dosage - 2.017 g/L; agitation speed - 120 rpm and contact time - 108 min. Before and after sorption, *Sargassum myriocystum* was characterized. Kinetic studies were performed using various kinetic models. It was found that the sorption process of Cr(VI) ions follows pseudo-second order, Elovich and power function kinetics. The data obtained were fitted to different isotherms. Sorption of Cr(VI) onto *Sargassum myriocystum* follows Langmuir and Toth isotherm models (R^2=0.993 and 0.992), with a maximum sorption capacity of 66.66 mg/g. The calculated thermodynamic parameters such as ΔG^o, ΔH^o and ΔS^o showed that the sorption of Cr(VI) ions onto *Sargassum myriocystum* biomass was feasible, spontaneous and endothermic. Desorption experiments show that the *Sargassum myriocystum* sorbent can be regenerated using 0.2 M HCl solutions with up to 80% recovery.

Keywords: Adsorption, Chromium (VI), RSM, Thermodynamics, Kinetics, Brown Algae

INTRODUCTION

Chromium and its compounds are ubiquitous and persistent environmental contaminants,released into the natural environment from a variety of anthropogenic sources, including the electroplating, leather tanning processes, chromite ore processing, wood preservation, alloys making, corrosion control, pigment and dyes, and metal finishing industries [1,2]. Cr(VI) is a carcinogenic and mutagenic metal [3], which may cause damage to the kidney, lungs and ulcerations to the skin [4]. Several international environmental agencies have introduced strict policy with regard to metal expulsion, especially from industrial activities. According to USEPA, the maximum permissible discharge of Cr(VI) into surface water is 0.5 mg/ L, while total Cr including Cr(III), Cr(VI) and its other forms is synchronized to below 2 mg/L [5]. The conventional physical-chemical methods for removal of heavy metals from effluents include precipitation, ion exchange, reverse osmosis, oxidation, which are, in some cases, highly expensive and ineffective at lower concentrations of metal ions [6,7].

Biosorption, known as the sorption of heavy metals onto biological materials, is becoming a potential alternative for toxic metal removal from water [8,9] and is a cost effective technology that uses readily available biomass from nature [10]. Among many sorbents, marine seaweeds are excellent sorbents for metals [11]. In recent years, the metal sorption potential of various red, green and brown seaweeds has been investigated by many researchers [12-14]. Seaweeds have a high bonding affinity with heavy metals [15-17]. Since their cell walls have different functional groups (such as carboxyl, hydroxyl, phosphate or amine) that can bind to metal ions [18], they are much more efficient than active carbon and natural zeolites, depending on the pH, these groups are either protonated or deprotonated [19,20]. The advantages of using dried aquatic algae for metal removal derive from its high efficiency as sorbents, easy handling, no nutrient requirements, low costs, and their availability. Research in the field of sorption has mostly concerned itself with brown algae [21-25].

In brown algae, the most abundant acidic functional group is the carboxylic. It constitutes the highest percentage of titratable sites, typically greater than 70%, in dried brown algal biomass. The sorption capacity of the algae is directly related to the presence of these sites on the alginate polymer, which itself comprises a significant component [26] of the dried seaweed biomass. Further, the majority of metals of interest (i.e. Cr^{3+}, Cd^{2+}, Co^{2+}, Cu^{2+}, Fe^{2+}, Ni^{2+}, Pb^{2+}) display maximal or near maximal sequestration at pHs near the apparent dissociation constant of carboxylic acids observed in brown algal biomass (pK0 near 5). The role of carboxylic groups in the adsorption process has been clearly demonstrated in earlier studies [27]. The second most abundant acidic functional group in brown algae is the sulfonic acid of fucoidan. Sulfonic acid groups typically play a secondary role, except when metal binding takes place at low pH. Hydroxyl groups are also present in all polysaccharides, but they are less abundant and only become negatively charged at pH>10, thereby, also playing a secondary role in metal binding at low pH [28].

†To whom correspondence should be addressed.
E-mail: harrishjk@rediffmail.com

So far, no study reports the usage of available using *Sargassum myriocystum* as sorbent for the removal of metals. Hence we used this marine macro brown algae as a sorbent for the removal of Cr(VI) from aqueous solution. The influence of various operating parameters such as pH, sorbent dosage, agitation speed and contact time on the sorption process of Cr(VI) onto the marine macro-algae *Sargassum myriocystum* was studied using a central composite design (CCD) method. The experimental data were analyzed in terms of kinetic and equilibrium isotherm models. The results at different temperatures were used to evaluate thermodynamic parameters. Fourier transform infrared spectroscopy (FTIR) and scanning electron microscope (SEM) were used to find the various functional groups present on the cell wall of the sorbent and the surface morphology of sorbent, respectively.

MATERIALS AND METHODS

1. Chemicals and Equipment

For the experimental studies, deionized double distilled water was used. HCl, NaOH and buffer solutions (E.Merck) were used to adjust the solution pH. A pH meter (Elico, L1-129) was used for pH measurements. Atomic absorption spectrophotometer (AAS) (Elico SL - 176) was used to determine the chromium concentration in the sample.

2. Sorbent Preparation

Sargassum myriocystum, marine brown algae was collected from the Mandapam coast, Ramanadhapuram district, Tamilnadu, India. The algae were washed with deionized water several times to remove the extraneous materials and salts, till the algae contained no dirt. The washed algae were dried in sunlight for 10 days. The dried algae were cut into small pieces and powdered using a domestic mixer. The structure of the marine algae was modified by adding 0.1 M HCl. The content was stirred at 200 rpm for 8.0 hr at room temperature. The acid treated algal biomass was then centrifuged and washed with the physiological saline solution and dried in an oven at 333.15 K. The dried sorbent was ground on an agate stone pestle mortar and sieved. In this work, the powdered raw and acid treated algae of 60 mesh particle size were used for sorption process.

3. Preparation of Metal Ion Solution

Chromium ion solution was prepared from analytical grade $K_2Cr_2O_7$ (Merck Ltd., India). 1,000 mg/L stock solution of Cr(VI) was prepared from $K_2Cr_2O_7$. From the stock solution, the working solutions were prepared by diluting it to appropriate volumes.

Wastewater from electroplating unit was collected from a small scale industry located at Chennai, Tamilnadu, India. The effluent was transported to the laboratory in plastic containers and stored at 4 °C for further use. The wastewater was brown color and had a pH of 2.16. From the table it was found that copper, iron, zinc and nickel were also present along with chromium in the wastewater. The wastewater was characterized according to APHA methods [29] and (Table 1).

Table 1. Characteristics of the Electroplating wastewater

Parameters	Characteristics
Colour	Dark brown
pH	2.16
Total dissolved solids	18,769 mg/L
BOD	347 mg/L
COD	1053 mg/L
Sulphate	288 mg/L
Phosphate	0.56 mg/L
Cr(VI)	116 mg/L
Copper	1.23 mg/L
Zinc	137 mg/L
Iron	6.35 mg/L
Nickel	24.13 mg/L

4. Sorption Experimental Procedure

Based on CCD, experiments were carried out in 250 ml Erlenmeyer flasks. 100 ml of 100 ppm Cr solution was taken in Erlenmeyer flasks. A known quantity of sorbent was added to it, based on the experimental design. The pH of the content was adjusted by adding acid or alkali as required. Then the content was agitated in an incubator shaker (LARK). After the completion of experiments, the samples were taken out and centrifuged in a centrifuge (REMI) at 10,000 rpm for 3 min. The supernatant was analyzed for metal concentrations in AAS. Experiments were carried out in triplicate and the average values are reported. The amount of adsorbed chromium per unit mass of adsorbent (q_e, mg/g) is obtained using the following expression:

$$q_e = \frac{(C_o - C_e)V}{m} \quad (1)$$

Whereas the amount of adsorbed chromium per unit mass of adsorbent at time t (q_t, mg/g) was obtained by using following expression:

$$q_t = \frac{(C_o - C_t)V}{m} \quad (2)$$

where, V is the volume of solution treated in liter, C_o is the initial concentration of chromium metal ion in mg/L, C_e is the equilibrium chromium metal ion concentration in mg/L, C_t (mg/L) is the concentration of adsorbents at time t, and m is the biomass in gram.

5. Experimental Design by RSM

RSM is a statistical tool used to find the optimal response within specific ranges of pre-established factors, through a second-order equation. In this study, CCD was used to study the effects of pH, sorbent dosage (g/L), agitation speed (rpm) and contact time (min) on Cr(VI) sorption. It also gives the linear, interactive and quadratic effects. The coded values of the process parameters are determined by the following equation:

Table 2. Experimental range and levels of independent process variables

Independent variable	Coded levels					
	Code	−2	−1	0	+1	+2
pH	A	3	4	5	6	7
Sorbent dosage (g/L)	B	1	1.5	2	2.5	3
Agitation speed (rpm)	C	40	80	120	160	200
Contact time (min)	D	60	80	100	120	140

Table 3. CCD based experimental design and its response for Chromium (VI) removal

Run order	(A) pH	(B) Sorbent dosage (g/L)	(C) Agitation speed (rpm)	(D) Contact time (Min)	Percentage Cr(VI) removal	
					Experimental	Predicted
1	1 (6)	−1 (1.5)	−1 (80)	−1 (80)	54.55	49.799
2	−1 (4)	1 (2.5)	1 (160)	−1 (80)	35.29	37.495
3	0 (5)	0 (2)	0 (120)	0 (100)	85.16	85.160
4	0 (5)	−2 (1)	0 (120)	0 (100)	35.29	35.776
5	0 (5)	0 (2)	0 (120)	0 (100)	85.16	85.160
6	0 (5)	0 (2)	2 (200)	0 (100)	54.28	57.871
7	1 (6)	−1 (1.5)	1 (160)	1 (120)	43.41	39.145
8	2 (7)	0 (2)	0 (120)	0 (100)	40.05	45.548
9	0 (5)	0 (2)	0 (120)	0 (100)	85.16	85.160
10	0 (5)	0 (2)	0 (120)	0 (100)	85.16	85.160
11	0 (5)	0 (2)	0 (120)	−2 (60)	55.55	63.090
12	0 (5)	0 (2)	0 (120)	0 (100)	85.16	85.160
13	−1 (4)	−1 (1.5)	−1 (80)	1 (120)	64.51	62.537
14	−1 (4)	1 (2.5)	1 (160)	1 (120)	61.26	58.657
15	0 (5)	0 (2)	−2 (40)	0 (100)	69.33	66.080
16	1 (6)	−1 (1.5)	−1 (80)	1 (120)	33.77	38.578
17	0 (5)	0 (2)	0 (120)	2 (140)	80.23	73.031
18	−1 (4)	1 (2.5)	−1 (80)	−1 (80)	49.36	46.270
19	0 (5)	0 (2)	0 (120)	0 (100)	85.16	85.160
20	−1 (4)	1 (2.5)	−1 (80)	1 (120)	50.44	59.230
21	−1 (4)	−1 (1.5)	−1 (80)	−1 (80)	60.18	64.860
22	1 (6)	1 (2.5)	−1 (80)	1 (120)	70.13	68.954
23	1 (6)	1 (2.5)	1 (160)	1 (120)	73.60	75.933
24	0 (5)	2 (3)	0 (120)	0 (100)	54.12	53.975
25	−1 (4)	−1 (1.5)	1 (160)	1 (120)	47.41	55.552
26	−1 (4)	−1 (1.5)	1 (160)	−1 (80)	55.85	49.672
27	1 (6)	1 (2.5)	−1 (80)	−1 (80)	66.02	64.892
28	1 (6)	−1 (1.5)	1 (160)	−1 (80)	43.94	42.163
29	−2 (3)	0 (2)	0 (120)	0 (100)	48.49	43.333
30	0 (5)	0 (2)	0 (120)	0 (100)	85.16	85.160
31	1 (6)	1 (2.5)	1 (160)	−1 (80)	69.05	63.669

$$X_i = \frac{(X_i - X_0)}{\Delta X} \quad (3)$$

where, x_i coded value of the i^{th} variable, X_i uncoded value of the i^{th} test variable and X_o uncoded value of the i^{th} test variable at center point. The range and levels of process variables are given in Table 2 and the experimental design is in Table 3. Regression analysis was performed to estimate the response function as a second order polynomial:

$$Y = \beta_0 + \sum_{i=1}^{k} \beta_i X_i + \sum_{i=1}^{k} \beta_{ii} X_i^2 + \sum_{i=1,\, i<j}^{k=1} \sum_{j=2}^{k} \beta_{ij} X_i X_j, \quad (4)$$

where, Y is the predicted response b_i, b_j and b_{ij} are coefficients estimated from regression; they represent the linear, quadratic and cross products of x_1, x_2 and x_3 on response.

A statistical program package, Design expert 7.1.5, was used for regression analysis of the data obtained and to estimate the coefficient of the regression equation. The equation was validated by ANOVA analysis. The significance of each term in the equation is to estimate the goodness of fit in each case. Response surfaces were drawn to determine the individual and interactive effects of test variable on percentage removal of Cr.

6. SEM and EDS Analysis

The micrographs were recorded using JEOL - scanning electron microscope model, JSM - 5610LV, with an accelerating voltage of 20 KV, at high vacuum (HV) mode and secondary electron image (SEI), an energy dispersive spectrum analyzer (EDS) attached to the SEM.

7. FT-IR Measurements

FT-IR spectra for both fresh and Cr(VI) treated *Sargassum myriocystum* were obtained by KBr pellets methods operated on FTIR spectrophotometer (Thermo Scientific -Nicolet iS_5 FTIR, USA) was used for the IR spectral studies (4,000-400 cm^{-1}) of sorbent. For IR spectral studies, 10 mg of sample was mixed and ground with 100 mg of KBr and made into pellet to investigate the functional groups present in the *Sargassum myriocystum* and to look into possible

Cr(VI) binding sites.

8. Desorption/Reuse Procedure

The recycling of sorbent is a most important aspect from the economical perspective. Hence, sorption-desorption experiments were carried out, up to ten cycles using 10 mL of 0.2 M HCl. A single cycle sequence consists of sorption followed by desorption (temperature - 308.15 K; sorbent dosage - 2.017 g/L; initial metal concentration - 100 mg/L; contact time - 108 min). To use the biomass for the next stage of cycle, the biomass was washed with excess of 0.2 M HCL solution and distilled water, sequentially.

$$\text{Desorption efficiency} = \frac{\text{Amount of metal ions desorbed}}{\text{Amount of metal ions adsorbed}} \times 100 \quad (5)$$

RESULTS AND DISCUSSION

1. Characteristics of Sorbent

The physical and chemical properties of the brown algae *Sargassum myriocystum* were determined by CHNSO analyzer [Perkin elmer, USA, Model - 2400 series ii]. The elemental analysis depicted the composition of sorbents as C - 22.6%; N - 6.07%; S - 2.54%. The apparent density of the sorbent was 1.31 g/cm^3. EDS analysis of sorbent before and after Cr(VI) sorption confirmed this observation. The humidity and the zeta potential were calculated as 1.39% and –0.054 V, respectively. The cell wall of brown algae contains three components: cellulose, the structural support; alginic acid, a polymer of mannuronic and guluronic acids and the corresponding salts of sodium, potassium, magnesium and calcium and sulfated polysaccharides. As a consequence, carboxyl and sulfate are the predominant active groups in this kind of algae [28]. The major functional groups that took part in adsorption are found to be -OH, C=O, C-O, C-H and -COOH. The functional group -SO_3^{2-} is additionally involved in adsorption with *Sargassum myriocystum*. The FTIR results show the presence of functional groups on the algal cell surfaces and also the mechanism of adsorption, which is dependent on functional groups especially hydroxyl, carboxyl, and carbonyl groups.

2. Effect of Sorbent Size

Before optimization, the effect of sorbent size (36, 60, 100 and 150 mesh) on Cr(VI) sorption by *Sargassum myriocystum* was studied. The sorbent was transferred to 250 mL Erlenmeyer flask containing 100 mL of Cr(VI) solutions and agitated at 120 rpm for a desired contact time. Then the sorbents were separated and the Cr(VI) concentration in the supernatant was analyzed by AAS. From Fig. 1(a), the Cr(VI) removal efficiency increased as the mesh size increased from 36 to 150 mesh because smaller particles provide larger surface area which results in higher removal efficiency. The maximum removal efficiency was attained for a mesh size of 150. But for regeneration process, the smaller size particles will not withstand the extreme conditions [30]. Hence 60 mesh particle size was selected for further studies.

3. Fitting Models

Sorption of Cr(VI) was carried out according to the CCD and the results obtained from experiments, along with the theoretically predicted responses, are given in Table 3. The response for the removal of chromium in terms of coded factors is given below:

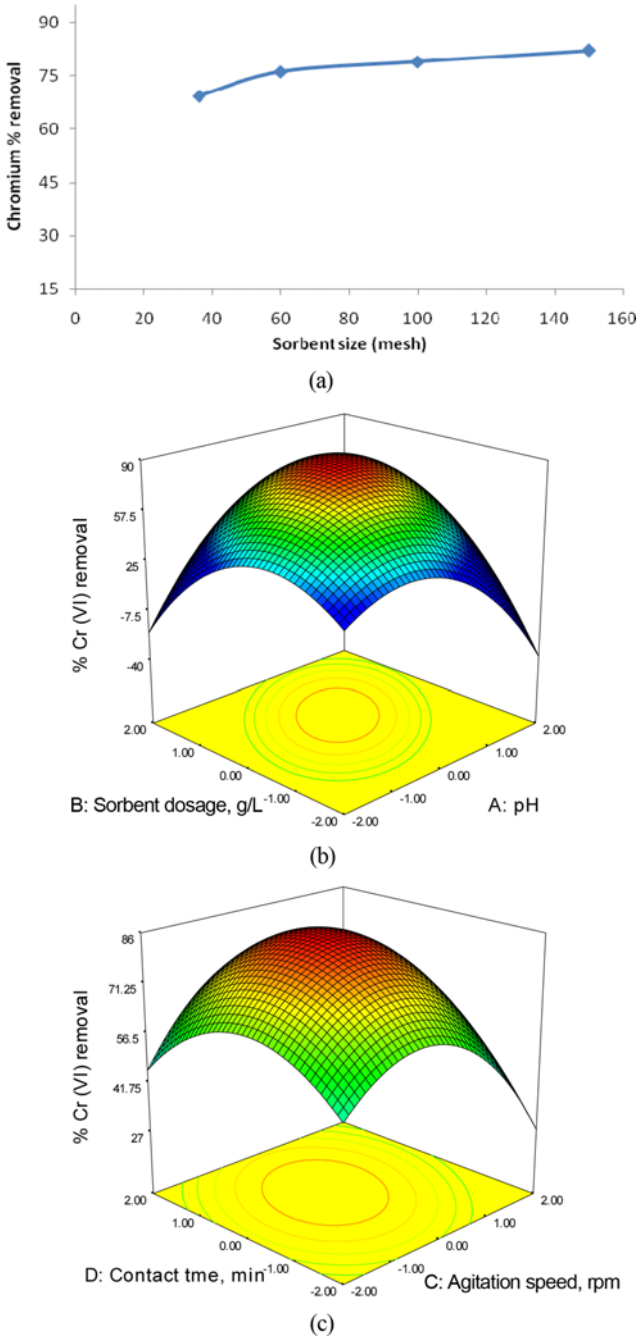

Fig. 1. (a) Effect of sorbent size on sorption of Cr(VI) on *Sargassum myriocystum*. Initial Cr(VI) conc.=50 mg/L, sorbent dosage=1 g/L, contact time=90 min, pH=5. (b) Interactive effect of pH and sorbent dosage on Cr(VI) removal by *Sargassum myriocystum*. (c) Interactive effect of agitation speed and contact time on Cr(VI) removal by *Sargassum myriocystum*.

$$\begin{aligned} Y = {} & 85.16 - 0.553750A + 4.54958B + 2.05208C + 2.48542D \\ & - 10.1799A^2 - 10.0711B^2 - 5.79615C^2 - 4.27490D^2 + 8.42063AB \\ & - 1.88812AC + 2.22438AD - 1.60313BC + 3.82063BD - 2.05062CD \end{aligned} \quad (6)$$

where, Y is the percentage removal of Cr(VI) and A, B, C and D are the coded values of pH, sorbent dosage (g/L), agitation speed (rpm) and contact time (min), respectively.

Table 4. ANOVA for Chromium (VI) removal using *Sargassum myriocystum*

Source	Sum of squares	df	Mean square	F-value	P-value prob>F
Model	8215.11	14	586.79	17.99	<0.0001
A - pH	7.36	1	7.36	0.23	0.6412
B - Sorbent dosage, g/L	496.77	1	496.77	15.23	0.0013
C - Agitation speed, rpm	101.07	1	101.07	3.10	0.0975
D - contact time, min	148.26	1	148.26	4.54	0.0489
AB	1134.51	1	1134.51	34.77	<0.0001
AC	57.04	1	57.04	1.75	0.2047
AD	79.17	1	79.17	2.43	0.1389
BC	41.12	1	41.12	1.26	0.2781
BD	233.55	1	233.55	7.16	0.0166
CD	67.28	1	67.28	2.06	0.1703
A^2	2963.39	1	2963.39	90.83	<0.0001
B^2	2900.41	1	2900.41	88.90	<0.0001
C^2	960.68	1	960.68	29.45	<0.0001
D^2	522.58	1	522.58	16.02	0.0010
Residual	522.00	16	32.63		
Lack of fit	522.00	10	52.20		
Pure error	0.000	6	0.000		
Cor total	8737.11	30			

Std. Dev - 5.71; R-squared - 0.9403; Mean - 61.68; Adj R-squared - 0.8880; C.V. % - 9.26
Pred R-squared - 0.7559; PRESS - 3006.73; Adeq Precision - 12.429

The test for significance of regression model and the results of ANOVA are given in Table 4. P value less than 0.05 indicates that the model terms are significant. Non-significant value lack of fit shows the validity of the quadratic model for the sorption of chromium by *Sargassum myriocystum*. The predicted R^2 and adjusted R^2 values 0.9403, 0.8880, respectively, indicate the better fitness of model with the experimental data. A low CV value, 9.26, indicates that the deviations between experimental and predicted values were low. Adeq precision measures the signal-to-noise ratio. A ratio greater than 4 is desirable. In this work, the ratio is found to be 12.429, which indicates an adequate signal [31]. The linear effect of B and D, square effect of A^2, B^2, C^2, D^2, and interactive effects of AB and BD were significant model terms for the sorption of Cr(VI). This implies that the linear effect of sorbent dosage, contact time and square effect of pH, sorbent dosage, agitation speed and contact time were more significant factors.

4. Effect of Variables on Cr(VI) Removal

The effect of process variables on sorption efficiency of *Sargassum myriocystum* is shown in Figs. 1(b)-1(c). It is evident that the sorption efficiency of Cr(VI) on *Sargassum myriocystum* depends on pH, sorbent dosage, agitation speed and contact time.

4-1. Effect of pH on Sorption

The pH of aqueous solution is an important environmental factor influencing not only site dissociation, but also the solution chemistry of the heavy metals. pH also strongly influences the speciation and sorption availability of the heavy metals [32]. In this study, Cr(VI) removal process was influenced significantly by variation of pH and the results are shown in Fig. 1(b). At pH 5.2, the removal percentage was 85.16%. As pH increased, the removal percentage decreased gradually. The removal percentage decreased gradually beyond a pH of 5.0. The pH dependence of Cr(VI) removal can be largely related to the type and ionic state of these functional groups and also the metal chemistry in solution [33]. Chromium exhibits different types of pH dependent equilibriums in aqueous solutions [34]. As pH is shifted, the equilibrium also shifts; at lower pH values (pH<2.0), $Cr_3O_{10}^{2-}$ and $Cr_4O_{13}^{2-}$ species are formed; at a pH range of 2-6, $HCrO_4^-$ and $Cr_2O_7^{2-}$ ions are in equilibrium. At pH>8.0, CrO_4^{2-} is the predominant species in the solution [34-36]. At lower pH, the negatively charged chromium species bind through electrostatic attraction to positively charged functional groups on the surface of biomass cell wall because more functional groups carrying positive charges would be exposed. As pH increased, the overall surface charge on cell walls became negative and biosorption decreased. On the other hand, the reduction process of hexavalent to trivalent chromium requires a large amount of protons [37].

4-2. Effect of Sorbent Dose

Fig. 1(b) shows the effect of sorbent dosage on the removal of Cr(VI). As can be seen from Fig. 1(b), the sorption of metal ions increases with increase in sorbent dosage from 1 to 2.017 g/L and decreases with further increase in sorbent dosage. Similar trends explained that as a consequence of partial aggregation of biomass at higher biomass concentration, which results in the decrease in effective surface area for the sorption [38].

4-3. Effect of Agitation Speed

The response surface plot for the effect of agitation speed (40-200 rpm) on Cr(VI) of *Sargassum myriocystum* sorbent is shown in Fig. 1(c). From the plot, a maximum sorption of Cr(VI) occurs at 136 rpm. At low agitation speed, the sorbent does not spread in the sample but remains accumulated. This may cover the active sites of the lower layer adsorbent, and only the upper layer adsor-

bent active sites adsorb the metal ion. Consequently, all the surface binding sites were readily available for metal uptake by applying sufficient agitation speed. At higher agitation speed, the percentage removal decreases. This is attributed to improper contact between the metal ions and the binding sites as the suspension is no longer homogeneous due to vortex formation, which makes the adsorption of Cr(VI) difficult [39].

4-4. Effect of Contact Time

Fig. 1(c) shows the interactive effect of agitation speed and contact time on the sorption of Cr(VI) on to the brown algae. It has been observed that the Cr(VI) removal efficiency was high initially and then slowly decreased till it reached the saturation level (108 min). Further increase in the contact time has a negligible effect on the sorption capacity of Cr(VI) sorption. This is due to larger surface area of the sorbent available for Cr(VI) sorption. But as time progresses, the sorbed Cr(VI) forms a monolayer and the vacant sites available on the *Sargassum myriocystum* becomes exhausted. At this stage, the removal rate is controlled by the rate at which the Cr(VI) ions are transported from the exterior to the interior sites of the sorbent. Also, the active sorption sites in a system are definite and each active site absorbs only one ion in a monolayer. The metal uptake by the sorbent surface will be rapid initially and slow down with the decreasing availability of active sites [40].

The second-order polynomial models obtained in this study were used to determine the optimum conditions. Optimum condition for the removal of Cr(VI) from aqueous solution using a brown algae *Sargassum myriocystum* is: Initial pH - 5.2, sorbent dosage - 2.017 g/L, agitation speed - 120 rpm and contact time - 108 min.

5. Effect of Temperature and Thermodynamic Study

The effect of the temperature on the sorption of Cr(VI) ions was studied in the temperature range of 293.15 K to 313.15 K. An increase in temperature from 293.15 K to 308.15 K increases the specific uptake to 48.4 mg/g of Cr(VI) by *Sargassum myriocystum*. Further increasing the temperature from 308.15 K to 313.15 K decreases the specific uptake from 48.4 mg/g to 46.97 mg/g of Cr(VI). This is probably caused by a change in the texture of the sorbent and a loss in the sorption capacity due to material deterioration [10].

The thermodynamic behavior of the sorption of Cr(VI) ions on *Sargassum myriocystum* from aqueous solution was investigated. The thermodynamic constants, free energy change (ΔG^o), enthalpy change (ΔH^o) and entropy change (ΔS^o) were calculated to evaluate the thermodynamic feasibility of the process and to confirm the nature of the adsorption process. The Gibbs adsorption process, free energy, as well as the enthalpy process was calculated from experimental results using the following equations:

$$\Delta G^o = -RT \ln K \quad (7)$$

$$\Delta G^o = \Delta H^o - T\Delta S^o \quad (8)$$

where, R is the universal gas constant (8.314×10^{-3} kJ/mol K), T is the temperature in Kelvin and K is the equilibrium constant, calculated as the surface and solution metal distribution ratio ($K=q_e/C_e$) [41]. From Fig. 2(a), the values of ΔH and ΔS were calculated from the intercept and slope of a plot of ΔG^o versus T according to Eq. (8) by linear regression analysis. The calculated thermodynamic parameters are listed in Table 5. Positive values of ΔH^o suggest the endothermic nature of the sorption and the negative values of ΔG^o indicate the spontaneous nature of the sorption process. However, the negative value of ΔG^o decreases with an increase in temperature, indicating that the spontaneous nature of sorption is inversely proportional to the temperature. Similar endothermic nature of the sorption process has been reported for other sorbent systems [42,43]. The increase in sorption with temperature may be attributed either to the increase in the number of active surface sites available for sorption on the adsorbent or due to the decrease in the boundary layer thickness surrounding the sorbent, so that the mass transfer resistance of sorbate in the boundary layer decreases [44]. The positive values of ΔS^o show the increasing ran-

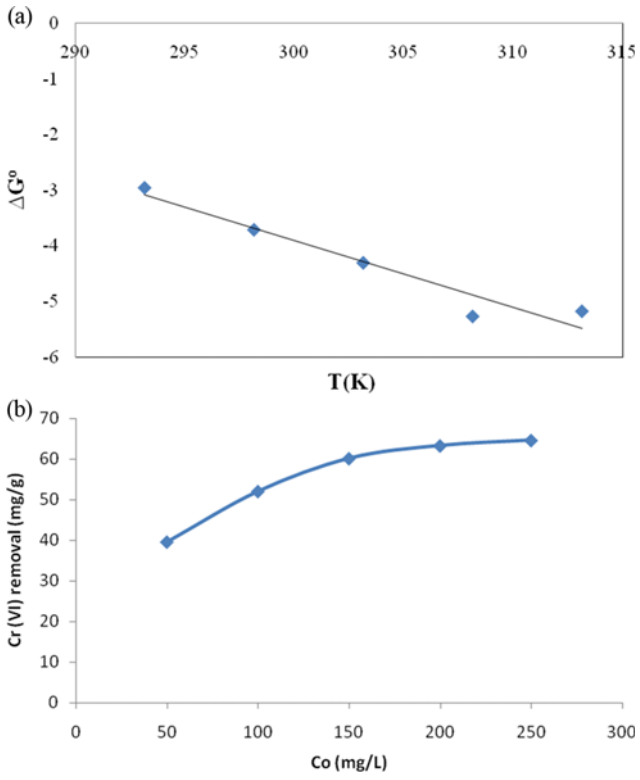

Fig. 2. (a) Plot of ΔG^o versus T for the estimation of thermodynamic parameters for sorption of Cr(VI) onto *Sargassum myriocystum*. (b) Removal efficiency of *Sargassum myriocystum* vs initial Cr(VI) concentration at pH - 5.2, temperature - 308.15 K, sorbent dosage - 2.017 g/L, agitation speed - 120 rpm and contact time - 108 min.

Table 5. Thermodynamic parameters for the Sorption of Cr(VI) on to *Sargassum myriocystum* at different temperatures

Metal ion	Temp. (K)	ΔG^o (kJ/mol)	ΔS (kJ/mol k)	ΔH (kJ/mol)
Cr(VI)	293.15	−2.9519	0.12	32.12
	298.15	−3.7069		
	303.15	−4.3019		
	308.15	−5.2669		
	313.15	−5.1742		

domness at the solid/solution interface during the sorption process.

6. Effect of Metal Ion Concentration

The effect of initial Cr(VI) metal ion concentration was investigated by varying initial Cr(VI) concentration from 50-250 mg/L at the optimized conditions (pH - 5.2, Temperature - 308.15 K, sorbent dosage - 2.017 g/L, agitation speed - 120 rpm and contact time - 108 min).The results showed that the metal uptake of *Sargassum myriocystum* increased with the increasing initial Cr(VI) concentration at the same process conditions (Fig. 2(b)). When the initial Cr(VI) concentration increased from 50 to 250 mg/L, the metal uptake increased from 39.57 mg/g to 64.60 mg/g. Similar results have been reported earlier [45-47]. The increase in Cr(VI) removal with the initial Cr(VI) concentration is due to higher availability of Cr(VI) ions in the solution, and also at lower initial Cr(VI) concentrations the ratio of the initial moles of metal uptake to the available surface area is low. The initial Cr(VI) concentration in the solution provides an important driving force to overcome mass transfer resistance of metal ions between the aqueous and solid phases [48].

7. Equilibrium Isotherm Study

The batch experimental data was applied to linear isotherms, namely, Langmuir, Freundlich, Dubinin Radushkevich, Temkin, Sips and Toth isotherms, to determine the mechanism of Cr(VI) sorption onto *Sargassum myriocystum*.

7-1. Langmuir Isotherm

Langmuir proposed a theory to describe the sorption of gas molecules onto metal surfaces [49]. The linear form of Langmuir isotherm is given by,

$$\frac{1}{q_e} = \frac{1}{q_m b C_e} + \frac{1}{q_m} \tag{9}$$

where, q_m is the monolayer sorption capacity of the sorbent (mg/

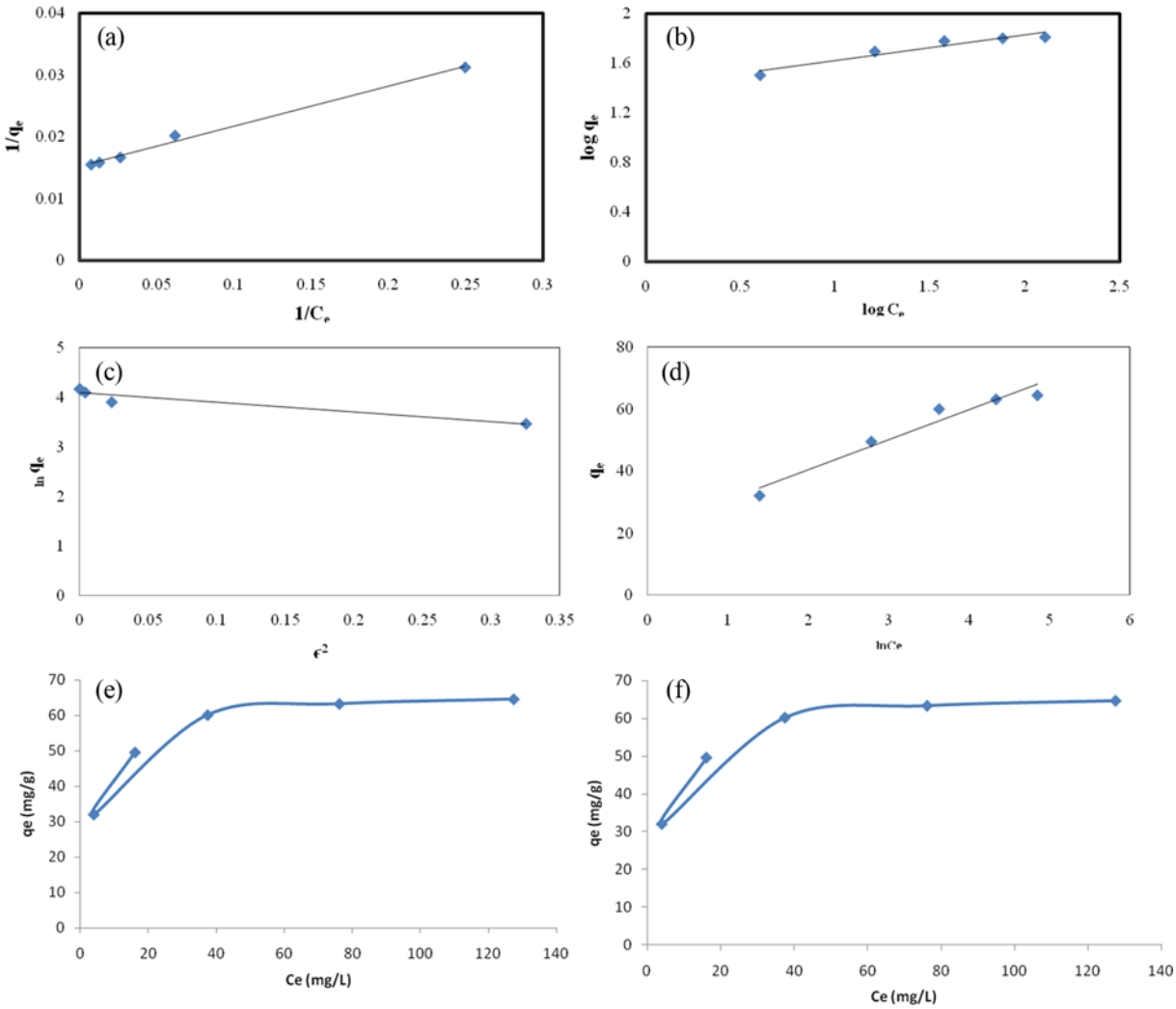

Fig. 3. (a) Langmuir isotherm plots for the sorption of Cr(VI) onto *Sargassum myriocystum* at 308.15 K temperature. (b) Freundlich isotherm plots for the sorption of Cr(VI) onto *Sargassum myriocystum* at 308.15 K temperature. (c) Dubinin-Radushkevich isotherm plots for the sorption of Cr(VI) onto *Sargassum myriocystum* at 308.15 K temperature. (d) Temkin isotherm plots for the sorption of Cr(VI) onto *Sargassum myriocystum* at 308.15 K temperature. (e) Sips isotherm plots for the sorption of Cr(VI) onto *Sargassum myriocystum* at 308.15 K temperature. (f) Toth isotherm plots for the sorption of Cr(VI) onto *Sargassum myriocystum* at 308.15 K temperature.

Table 6. Langmuir, Freundlich, Dubinin-Radushkevich, Temkin, Sips and toth constants for the sorption of Cr(VI) on to *Sargassum myriocystum*

Sl. no	Isotherm model	Parameters	Cr(VI) sorption at temperature 308.15 K
1.	Langmuir	q_{max}	66.66 mg/g
		B	0.2307
		R^2	0.993
2.	Freundlich	K_f	25.94
		1/n	0.206
		R^2	0.919
3.	Dubinin-Redushkevich	q_{max}	60.09
		B	1.965
		E	0.5044
		R^2	0.913
4.	Temkin	B	9.71
		K_T	8.6581
		R^2	0.951
5.	Sips	a_s	3.328
		K_s	17.72
		Bs	0.2517
		R^2	0.779
6.	Toth	q_{max}	62.67
		nT	0.9715
		b_T	0.2675
		R^2	0.992

g), q_e is the equilibrium metal ion concentration on the sorbent (mg/g), C_e is the equilibrium metal ion concentration in the solution (mg/L), and b is the Langmuir sorption constant (L/mg) related to the free energy of sorption. Fig. 3(a) shows the Langmuir plots of Cr(VI) sorption isotherms for *Sargassum myriocystum* at different initial metal concentration. The constants q_m and b are tabulated in Table 6. Affinity between sorbent and sorbate was represented by the constant b. In general, good sorbents have a high q_{max} and a high R^2 (0.993). *Sargassum myriocystum* have high saturation (q_{max}) for different initial metal concentration of Cr(VI). Table 7 represents the comparison of sorption capacity (q_m; mg/g) of *Sargassum myriocystum* for Cr(VI) with that of various sorbents reported in the literature [42,50-74]. Based on the results, *Sargassum myriocystum* has very good potential for the removal of Cr(VI) from aqueous solution.

7-2. Freundlich Isotherm

The Freundlich isotherm is an empirical equation used to describe heterogeneous systems [75]. The linear form of Freundlich isotherm is represented by the equation

$$\log q_e = \log K_f + \frac{1}{n}\log C_e \tag{10}$$

Fig. 3(b) shows the Freundlich plots of Cr(VI) sorption isotherms for *Sargassum myriocystum* at different initial metal concentration, and the constants K_f and 1/n are given in Table 6. The values of K_F and 1/n were calculated from the intercept and slope of the plot between log q_e versus log C_e. K_f is a constant relating the sorption capacity and 1/n is an empirical parameter relating the sorption intensity, which varies with the heterogeneity of the material. From the graphs, K_f value was found to be 25.94 and 1/n value was 0.206. Usually, 1/n values between 0 and 1 indicate good sorption. In this work, a value of 0.206 indicates that the sorption of Cr(VI) onto the *Sargassum myriocystum* was favorable. In this case, the Langmuir equation fits the experimental data better than the Freundlich equation. This isotherm does not predict any saturation of the adsorbent by the sorbate. Instead, heterogeneous surface condition is predicted, indicating multilayer sorption on the surface.

7-3. Dubinin-Radushkevich Isotherm

The linear form of the D-R isotherm equation [76] is:

$$\ln q_e = \ln q_m - \beta_1 \varepsilon^2 \tag{11}$$

where, q_e is the amount of metal ions adsorbed on per unit weight of biomass (mg/g), q_m is the maximum sorption capacity (mg/g), β_1 is the activity coefficient related to sorption mean energy (mol^2/kJ^2) and ε is the Polanyi potential described as

$$\varepsilon = RT\ln\left(1+\frac{1}{C_e}\right) \tag{12}$$

where, R is the gas constant 8.314×10^{-3} kJ/mol K, T is the temperature in Kelvin and C_e is the equilibrium concentration of the Cr(VI) in solution (mg/L). The mean free energy of sorption per molecule of sorbate required to transfer one mole of ion from the infinity in the solution to the surface of biomass and can be determined by the following, Eq. (13):

$$E = \frac{1}{\sqrt{-2\beta_1}} \tag{13}$$

Fig. 3(c) shows the plot of $\ln q_e$ versus ε^2, from which the Dubinin-Radushkevich constants β_1 and q_m were calculated from the slope and intercept. The results are given in Table 6. The energy values obtained (Table 6) have E<8 kJ/mol, which indicates that all metal cation adsorptions are physical processes, since a chemical adsorption process has an E>8 kJ/mol [77,78]. From R^2 values, it is concluded that the sorption of Cr(VI) onto *Sargassum myriocystum* followed the Langmuir model. The sorption capacity was lower than the Langmuir model, which may be attributed to different assumptions taken into consideration.

7-4. Temkin Isotherm

The Temkin isotherm [79] has been used in the following form

$$q_e = \frac{RT}{b}\ln K_T + \frac{RT}{b}\ln C_e \tag{14}$$

$$q_e = B\ln K_T + B\ln C_e \tag{15}$$

where, constant B=RT/b, which is related to the heat of sorption, R is the universal gas constant (KJ/mol K), T is the temperature (K), b is the variation of sorption energy (J/mol) and K_T is the equilibrium binding constant (L/mg) corresponding to the maximum binding energy. Fig. 3(d) shows the plot of q_e versus $\ln C_e$, the isotherm constants were found and given in Table 6. The correlation factors show that the Langmuir model approximations to the experimental results are better than that of the Temkin model. Consequently, among the four isotherm models used, the Langmuir model offers the best correlation factors.

Table 7. Comparison of sorption capacity of different sorbents for Cr(VI) removal

Name of algae	Sorption capacity	Reference
Padina boergesenli (B)	49 mg/g	[42]
Padina (B)	54.6 mg/g	[50]
Sargassum (B)	31.7 9 mg/g	[50]
Sargassum sp. (B)	68.94 mg/g	[51]
Sargassum sp. (B)	65 mg/g	[52]
Sargassum siliquosum (B)	66.4 mg/g	[53]
Cystoseira indica (B)	20.9-27.9 mmol/g	[54]
Turbinaria ornate (B)	65%	[55]
Chlamydomonas Reinhardetti (G) (heat inactivated)	25.60 mg/g	[56]
Chlamydomonas Reinhardetti (G) (acid treated)	21.20 mg/g	[56]
Ulva lactuca (G)	27.60 mg/g	[57]
Ulva spp. (G)	30.20 mg/g	[57]
Fucus spiralis (B)	5.40 mg/g	[57]
Palmaria palmate (R)	33.80 mg/g	[57]
Aeromonas caviae (G)	124.46 mg/g	[58]
Scenedesmus obliquus (G)	58.80 mg/g	[59]
Spirogyra spp. (G)	14.7 mg/g	[60]
Ecklonia (B)	94%	[61]
Ceramium virgatum (R)	26.5 mg/g	[62]
Sargassum spp. (B)	19.06 mg/g	[63]
Sargassum spp. (B) (Raw)	0.601 mmol/g	[64]
Sargassum spp. (B) (acid treated)	1.123 mmol/g	[64]
Laminaria japonica (B)	62.18 mg/g	[65]
Porphypa yezoensis ueda (R)	60.60 mg/g	[65]
Spirulina platensis (BGA)	99%	[66]
Cladophora albida (G)	41.70 mg/g	[67]
Yarrowia lipolytica (Marine Isolate)	63.73 mg/g	[68]
Sargassum filipendula (B)	0.819 mmol/g	[69]
Laminaria digitata (B)	2.10 mmol/g	[70]
Activated alumina	25.57 mg/g	[71]
Fly ash	23.86 mg/g	[71]
Red mud	0.436 mmol/g	[72]
Acid activated clay	83 mg/g	[73]
Turkish brown coal	11.2 mmol/g	[74]
Sargassum myriocystum (B)	66.66 mg/g	Present study

7-5. Sips Isotherm

Sips (1948) proposed a model that has a similar form to the Freundlich isotherm, differing only on the finite limit of adsorbed amount at sufficiently high concentration.

$$q_e = \frac{K_s C_e^{\beta s}}{1 + a_s C_e^{\beta s}} \tag{16}$$

whereis βs the parameter characterizing the system's heterogeneity, which may be due to the sorbent or the heavy metal, or a combination of both. All the Sips parameters, a_s, K_s and βs, are governed by operating conditions such as pH and temperature. The results obtained from the model are shown in Fig. 3(e) and in Table 6. For the sorption of Cr(VI) on *Sargassum myriocystum*, the parameter βs is close to unity [80], but the correlation coefficient is very low.

7-6. Toth Isotherm

Toth equation is expressed as [81]

$$q_e = q_{max} \frac{b_T C_e}{(1 + (b_T C_e)^{nT})^{1}/nT} \tag{17}$$

Toth equation possesses the correct Henry law type limit besides a parameter to describe the heterogeneities of the system. The Toth model is shown in Fig. 3(f) and the results are tabulated in Table 6. However, this equation is unable to predict the isotherm in a particular heterogeneous system as illustrated in the sorption of Cr(VI) into *Sargassum myriocystum.*

7-7. Sorption Separation Factor

The effect of isotherm shape can be used to predict whether an adsorption system is "favorable" or "unfavorable" [82]. According to Hall et al. [83], the essential features of the isotherm can be ex-

Table 8. Separation factor and their condition to find the feasibity and type of isotherm

Type of Isotherm	K_R	Condition
Langmuir	0.041	Favorable
Freundlich	0.00038	Favorable
Dubinin-Redushkevich	0.0050	Favorable
Temkin	0.0011	Favorable
Sips	0.00056	Favorable
Toth	0.036	Favorable

pressed in terms of a dimensionless constant separation factor or equilibrium parameter K_R (Supplementary data), which is defined by the following relationship:

$$K_R = \frac{1}{1 + K_a C_O} \quad (18)$$

where, K_R is a dimensionless separation factor, C_O is initial metal concentration (mg/L) and K_a is isotherm constant (L/mg). From the K_R values in Table 8, it is found that all isotherms are favorable. High value of K_R, shows that the Langmuir isotherm fits better than all other isotherm.

8. Sorption Kinetics

The contact time studies provide information about the minimum time required to bind the maximum amount of Cr(VI) ions at the liquid-solid interface, and thus help in scaling up the process. The optimum (equilibrium) time helps in studying the rate of the binding process. Several kinetic models are needed to establish the mechanism of a sorption process. To investigate the kinetics of the sorption of Cr(VI) on *Sargassum myriocystum*, five kinetic models were employed: pseudo-first-order, pseudo-second-order, intra particle diffusion, power function and Elovich model.

8-1. Pseudo-first-order Model

Lagergren suggested a pseudo-first-order equation for the sorption of a liquid/solid system based on the solid capacity [84]. The

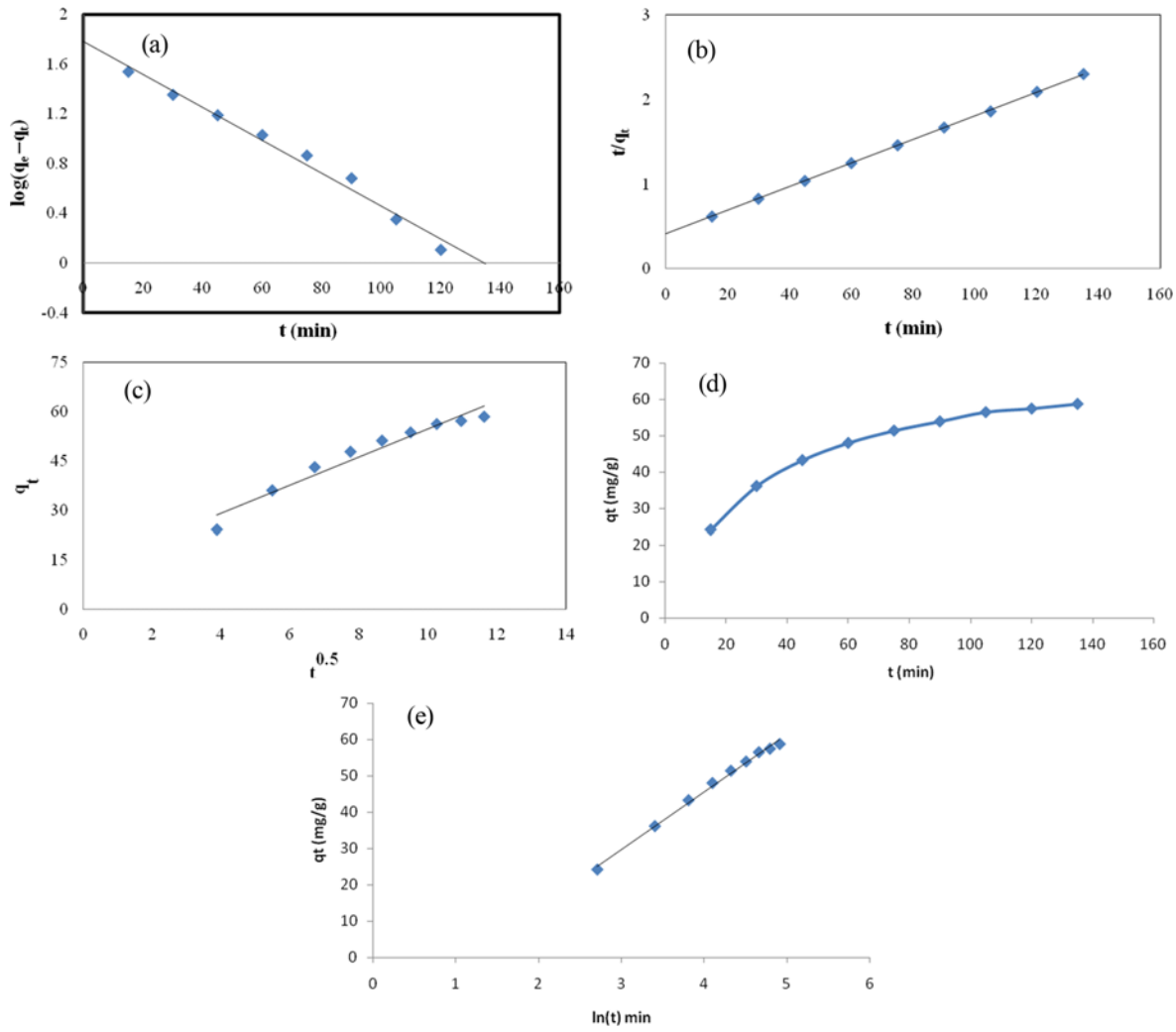

Fig. 4. (a) Pseudo first order plots for the sorption of Cr(VI) onto *Sargassum myriocystum*. (b) Pseudo second order plots for the sorption of Cr(VI) onto *Sargassum myriocystum*. (c) Intra particle diffusion model plots for the sorption of Cr(VI) onto *Sargassum myriocystum*. (d) Power function model plots for the sorption of Cr(VI) onto *Sargassum myriocystum*. (e) Elovich model plots for the sorption of Cr(VI) onto *Sargassum myriocystum*.

Table 9. Kinetic parameters obtained from various kinetic models for Cr(VI) on to *Sargassum myriocystum*

Sl. no	Kinetic model	Parameters	Cr(VI) sorption at temperature 308.15 K
1.	Pseudo first order	K_1 (min^{-1})	0.029
		R^2	0.983
2.	Pseudo second order	K_2 ((g/mg)min)	0.000474
		R^2	0.999
3.	Intra particle diffusion	K_{id} ((mg/g)$min^{-0.5}$)	4.308
		R^2	0.950
4.	Power function	K	10.69
		V	0.3555
		R^2	0.988
5.	Elovich	A	5.1356
		B	0.0628
		R^2	0.995

linear form of the pseudo first-order rate equation is given as follows:

$$\log(q_e - q_t) = \log q_e - \frac{K_1}{2.303}t \quad (19)$$

where q_t and q_e (mg/g) were the amounts of the Cr(VI) ions sorbed at equilibrium (mg/g) and t (min), respectively, and K_1 is the rate constant of the equation (min^{-1}). The sorption rate constants (K_1) can be determined experimentally by plotting log ($q_e - q_t$) versus t. It is shown in Fig. 4(a) and the values are reported in Table 9.

8-2. Pseudo-second-order Model

The pseudo-second-order model predicts the sorption behavior over the whole time adsorption [85]:.

$$\frac{t}{q_t} = \frac{1}{K_2 q_e^2} + \frac{1}{q_e}t \quad (20)$$

where, K_2 (g/mg min) is the rate constant of the second-order equation, q_t (mg/g) is the amount of sorption time t (min) and q_e is the amount of sorption equilibrium (mg/g). In Fig. 4(b), sorption rate constants (K_2) can be determined experimentally by plotting of t/q_t versus t. The rate constants and R^2 values are given in Table 9. However, the correlation coefficients, R^2, showed that the pseudo-second-order model fits better with the experimental data than the pseudo-first-order model.

8-3. Intraparticle Diffusion

Weber's intraparticle diffusion model [86] is defined by the following equation:

$$q_t = K_{id}t^{0.5} + C \quad (21)$$

where K_{id} is the intraparticle diffusion rate constant (mg/(g $min^{-0.5}$)) and C is the intercept. It was concluded that the sorption process of Cr(VI) on *Sargassum myriocystum* is comprised of three phases, suggesting that the intraparticle diffusion is not the rate-limiting step for the whole reaction. The uptake rate was initially very fast, then medium, finally giving way to slow uptake. The rate constants of intraparticle diffusion were calculated from Fig. 4(c). The values for all the kinetic models were calculated and summarized in Table 9. Pseudo-second-order model has higher correlation coefficient values, indicating that the sorption of Cr(VI) on the sorbent follows second-order kinetic model. Higher values of R^2 show a better fitness of the sorption data [87,88].

8-4. Power Function Model

The power function model is expressed as

$$q = Kt^{v} \quad (22)$$

where, q is amount of sorbate per unit mass of sorbent at time t, K and v are constants and v is positive and <1. Eq. (22) is empirical, except for the case where v=0.5, when it is similar to the parabolic diffusion equation. The constants of power function were calculated from Fig. 4(d). The values for all the kinetic models were calculated and summarized in Table 9. Based on the higher correlation coefficient value, the sorption of Cr(VI) on the sorbent follows the power function kinetic model.

8-5. Elovich Model

The Elovich Eq. (23) [89] incorporates α as the initial adsorption rate (mg/g min) and β (g/mg) as the desorption constant. This relates the extent of the surface coverage and activation energy for chemisorptions.

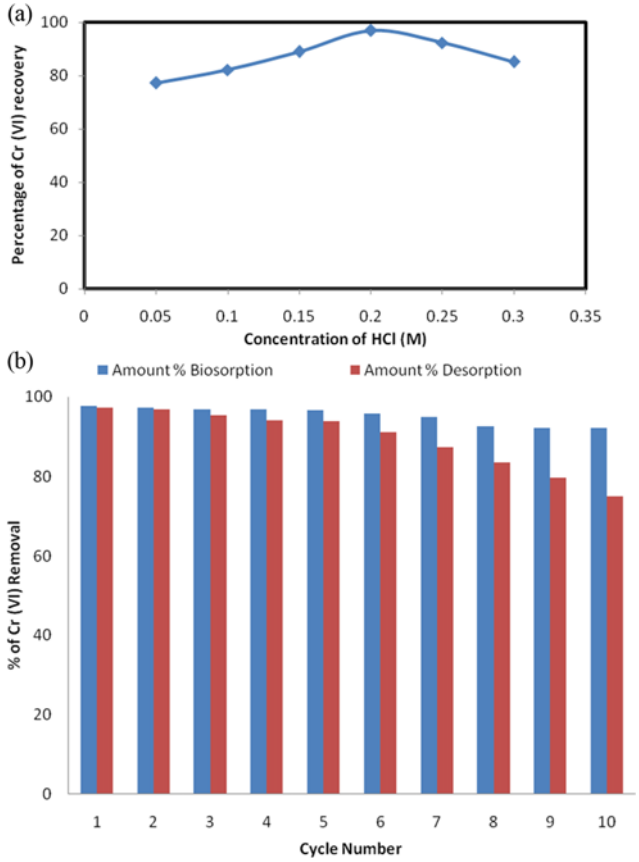

Fig. 5. (a) Desorption efficiency with different concentration of HCl (biomass concentration: 2.017 g/L; contact time: 108 min; temperature: 308.15 K). (b) Biosorption-desorption efficiency with cycle number (biomass concentration: 2.017 g/L; contact time: 108 min; temperature: 308.15 K).

$$\frac{dq}{dt} = \alpha e_t^{-\beta q} \quad (23)$$

Eq. (23) can be simplified to Eq. (24) by considering, $\alpha\beta >> t$ and by applying the boundary conditions $q_t=0$ at t=0 and $q_t=q_t$ at t=t

$$q_t = \frac{1}{\beta}\ln(\alpha\beta) + \frac{1}{\beta}\ln(t) \quad (24)$$

where, q_t is the amount of gas chemisorbed at time t. From the results (Table 9), the Cr(VI) sorption on brown algae fits the Elovich model [90]. A plot of q_t vs ln(t) (Fig. 4(e)) gives a linear relationship with a slope of $(1/\beta)$ and an intercept of $(1/\beta)\ln(\alpha\beta)$.

9. Desorption and Regeneration Studies

In the sorption process, to decrease the processing cost and to open the possibility of recovering the metal extracted from the liquid phase, it is desirable to regenerate the sorbent material. To investigate desorption of metal ion from metal loaded *Sargassum myriocystum*, the metal loaded sorbent was treated with HCl, which has

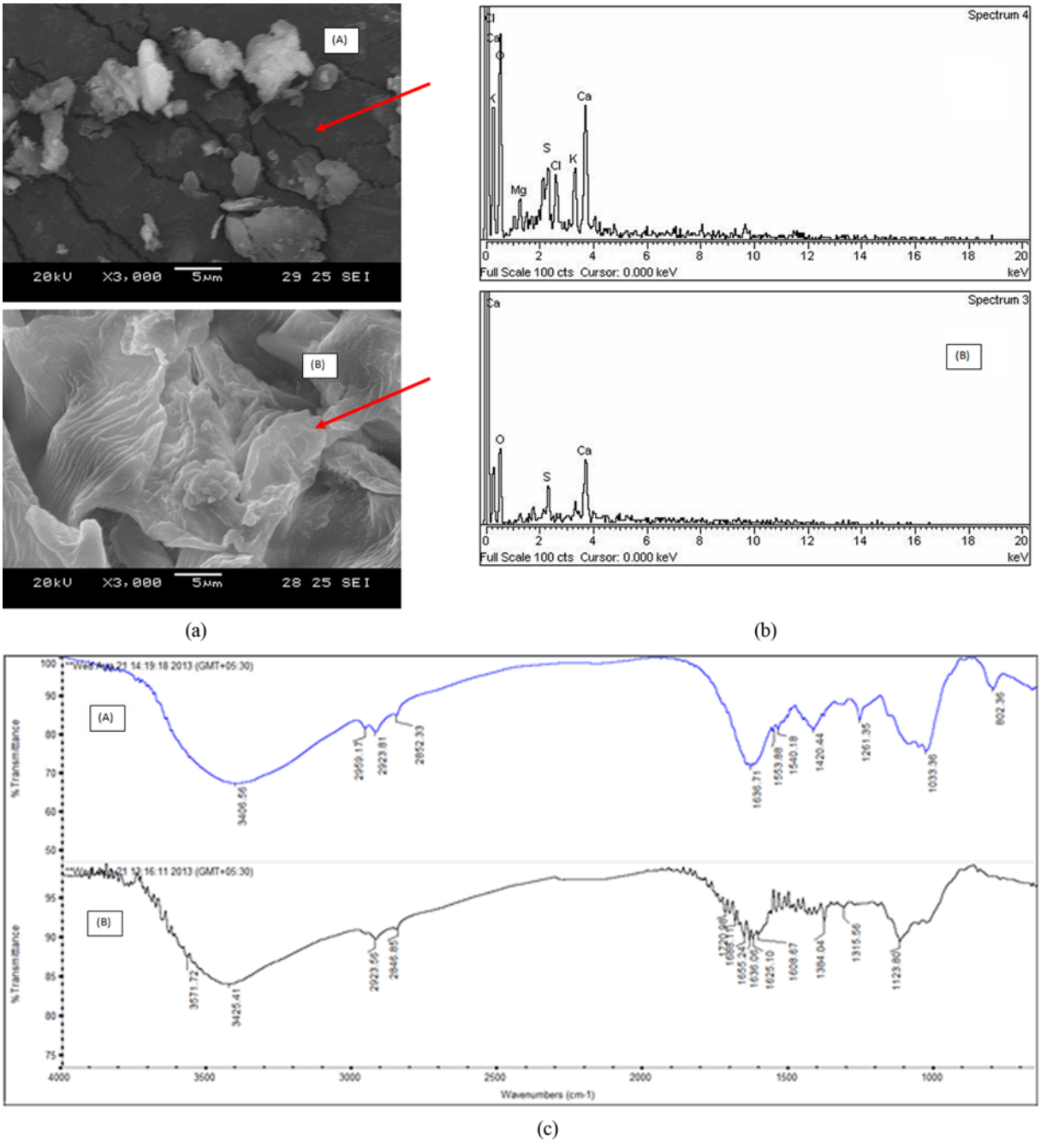

Fig. 6. (a) SEM images for Cr(VI) on *Sargassum myriocystum* (A) before adsorption (B) after adsorption. (b) EDS images for Cr(VI) on *Sargassum myriocystum* (A) before adsorption (B) after adsorption. (c) FTIR images for Cr(VI) on *Sargassum myriocystum* (A) before adsorption (B) after adsorption.

been reported as an efficient metal desorbent [21,91,92]. Desorption studies were performed with different HCl concentrations and the results are shown in Fig. 5(a). From our results, with the increasing of hydrochloric acid concentration, the desorption rate also increased initially, and then became almost stable. The maximum percentage recovery of Cr(VI) is 97.21% with 0.2 M HCL solution.

We performed repeated batch operations to examine the reusability of the algae biomass *Sargassum myriocystum* for Cr(VI) uptake. The Cr(VI) ions adsorbed onto biosorbents were eluted with 0.2 M HCL. A maximum of 97.21% of the adsorbed Cr(VI) ions was desorbed from the biosorbents in the first cycle. To show the reusability of the biosorption, adsorption-desorption cycles of Cr(VI) were repeated ten times by the test algae biomass. In Fig. 5(b), there was a gradual decrease in Cr(VI) sorption with an increase in the number of cycles. After a sequence of ten cycles, the Cr(VI) removal efficiency of the sorbent was reduced from 97.70% to 92.21%. The loss in the sorption capacity of the biomass for metal ions is found to be 5.49%. This might be due to the ignorable amount of biomass lost during the sorption-desorption process. These results show that the *Sargassum myriocystum* could be repeatedly used for ten cycles with little loss in their initial adsorption capacities.

10. SEM with EDS

SEM images were used for the surface analysis of *Sargassum myriocystum* as shown in Fig. 6(a). These figures demonstrate the fibrous superficial structure of the algal biomass surface where the metal cations could be adsorbed. The EDS images for the seaweed before and after adsorption are presented in Fig. 6(b) and show the elements present on the algae surface.

11. FTIR Study

The infrared (IR) spectrum obtained from FTIR of the *Sargassum myriocystum* is shown in Fig. 6(c). It displays a number of absorption peaks, indicating the complex nature of the examined biomass. The results revealed sorbent heterogeneity, evidenced by different characteristic peaks. The infrared absorption wavelengths of each peak and the corresponding functional groups are presented in Table 10 for *Sargassum myriocystum*. As seen in Table 11, the major functional groups that took part in sorption were -OH, C=O, C-O, C-H and -COOH. The functional group $-SO_3^{2-}$ is additionally involved in sorption with *Sargassum myriocystum*.

Table 11. Cost Analysis for sorption-desorption of Cr (to treat 1 L of Cr solution)

Description	Amount of chemical substance (g or L)	Current cost (Rs)
Marine algae (*Sargassum myriocystum*)	2.017 g	Rs.0.4034/-
Hydrocholoric acid (HCl)	0.01 L	Rs. 0.0854/-
	Total cost	Rs.0.4-0.6/-
Activated charcoal	1.850 g	Rs.1.0175/-
Hydrocholoric acid (HCl)	0.01 L	Rs. 0.0854/-
	Total cost	Rs.1-1.5/-

12. Sorption of Cr(VI) by Acid Treated Sorbent

Acid treatment is done for washing the cell wall to enhance uptake capacity of biomass by increasing the surface area and porosity of original sample [93-97]. The increase in metal uptake in sorption is due to the protonation of functional groups at low pH condition, giving an overall positive charge to the biomass, which adsorbed negatively anionic metal ions like CrO_4^{2-} [98]. The results obtained for the sorption of Cr(VI) using raw and acid treated *Sargassum myriocystum* are shown in Fig. 7(a). From the figure it is inferred that a maximum of 98.69% and 97.75% Cr removal was achieved by the acid treated and raw algae, respectively. From the figure, also, the Cr removal is higher for acid-treated algae. This is due to the cleavage of functional groups present in the sorbent material [99]. The finding is well supported by Mehta et al. [100] and Kalyani et al. [101] as these authors, respectively, noted a 39% and 70% increase in the metal binding capacity of biomass following HCl pretreatment. Singh et al. [102,103] also found improvement in Cu(II) and Pb(II) sorption ability of *Spirogyra neglecta* and *Pithophoraoedogonia* after HCl pretreatment.

13. Sorption of Cr(VI) from Electroplating Wastewater

The results obtained from the sorption of Cr from electroplating industry wastewater using acid treated *Sargassum myriocystum* are shown in Fig. 7(b). From the figure, it is inferred that a maximum of 89.17% Cr removal was achieved by the algae. Also,

Table 10. FTIR spectral characteristics of *Sargassum myriocystum* before and after sorption of Cr(VI)

Wavelength range (cm^{-1})	*Sargassum myriocystum*			Assignment
	Before loading of Cr(VI)	After loading of Cr(VI)	Differences	
3500-3000	3406.56	3425.41	+18.85	Bonded -OH groups
2900-2800	2959.17	2923.56	−35.61	CH stretching
	2852.33	2846.85	−5.48	
1740-1680	-	1720.98	-	C=O carbonyl groups
	1636.71	1655.24	+18.53	
	1553.88	1625.10	+71.22	
1500-1400	1540.18	1608.67	+68.49	C-O stretch
	1420.44	1384.04	−36.40	
1280-1240	1261.35	1315.56	+54.21	$-SO_3^{2-}$ stretching
1150-950	1033.36	1123.80	+100.44	$-PO_4^{3-}$ stretching
650-480	802.36	-	-	N - containing bioligands

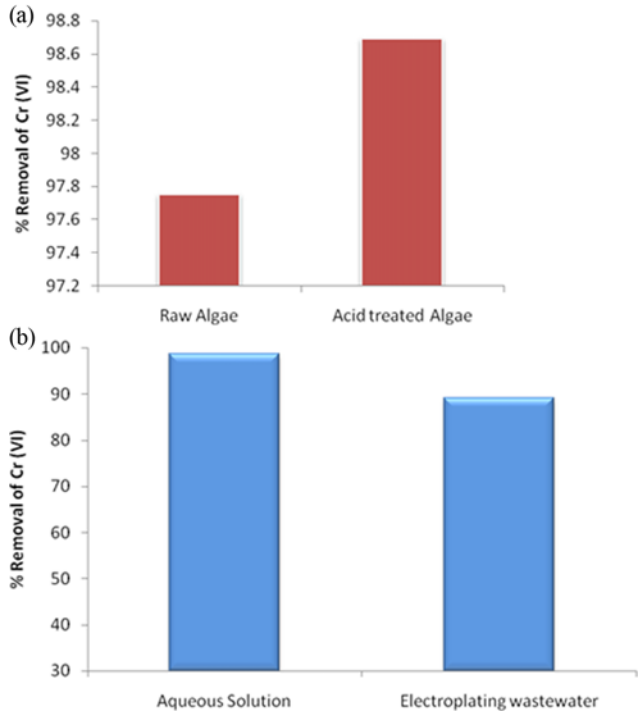

Fig. 7. (a) Removal percentage of Cr(VI) from aqueous solution using raw and acid treated algae (*Sargassum myriocystum*). (b) Removal percentage of Cr(VI) from aqueous solution and electroplating wastewater using acid treated algae (*Sargassum myriocystum*).

Cr removal was found to be higher for aqueous solution, than the electroplating wastewater. The decrease in Cr removal in electroplating wastewater may be due to the presence of other metal ions like Cu, Zn, Fe and Ni present in the wastewater, as indicated in Table 1, which occupies the sorption sites. In the aqueous sample of potassium dichromate, only Cr(VI) metal ions were present, so the binding sites on adsorbent surface were occupied by the single metal ions, but in a complex industrial wastewater, where more than one metal ion species are present. Hence Cr removal is higher in aqueous solution [99,104].

ECONOMIC ANALYSIS

We also did a cost analysis for the sorption of chromium. The total cost for the sorption of chromium using the marine brown algae *Sargassum myriocystum* was compared with the conventional activated charcoal using the standard cost analysis method [105]. According to the results given in Table 11, the total cost for the removal of chromium per liter of effluent by the activated charcoal was found to be Rs.1-1.50. But the cost for the removal of chromium using the brown marine algae was in the range of Rs.0.4-0.6, which is 60% less than the activated charcoal. Therefore, the marine sorbent is inexpensive when compared to activated charcoal.

CONCLUSION

We studied *Sargassum myriocystum* for the removal of toxic metal Cr(VI) ions from aqueous and electroplating wastewater. RSM was used to optimize the operating conditions and maximize the Chromium(VI) removal. From the results, the initial pH significantly influenced metal uptake. Sorption kinetics follows a pseudo-second-order, Elovich and power function models. Experimental data were analyzed using Langmuir, Freundlich, Dubinin-Radushkevich, Temkin, Sips and Toth isotherm models and found that the Langmuir and Toth model presented a better fit. SEM-EDS confirmed the presence of Cr(VI) ions on the biomass surface. Temperature affects the sorption process and the thermodynamic parameters show the spontaneous character of the sorption reaction. The maximum percentage removal of acid treated 98.69% and untreated algae biomass 97.75% was found to have higher chromium removal when compared to other similar sorbents. A 0.2 M HCl efficiently desorbed metal from the metal-loaded biomass during successive sorption/desorption cycles. The reusability of the sorbent was good after ten consecutive adsorption-desorption cycles without any considerable loss in sorption capacity. The results of this study form the basis for the development of cheaper sorbent and robust indigenous technology for sorption of Cr(VI) from aqueous and industrial waste water solutions.

SUPPORTING INFORMATION

Additional information as noted in the text. This information is available via the Internet at http://www.springer.com/chemistry/journal/11814.

NOMENCLATURE

RSM : response surface methodology
FTIR : fourier transform infrared spectroscopy
SEM : scanning electron microscope
USEPA : united states of environmental protection agency
CCD : central composite design
AAS : atomic absorption spectrophotometer
EDS : energy dispersive spectrum
X_i : uncoded value of the i^{th} test variable
X_o : uncoded value of the i^{th} test variable at center point
ΔG^o : gibbs free energy change
ΔH^o : enthalpy change
ΔS^o : entropy change
K : equilibrium constant
q_e : amount of adsorbed Chromium per unit mass of adsorbent [mg/g]
q_t : amount of adsorbed Chromium per unit mass of adsorbent at time t [mg/g]
C_o : initial concentration of Chromium metal ion [mg/L]
C_e : equilibrium Chromium metal ion concentration [mg/L]
C_t : concentration of metal ion at time t [mg/L]
V : volume of solution treated [L]
M : amount of biomass [gm]
q_m : maximum sorption capacity of the sorbent [mg/g]
b : Langmuir sorption constant [L/mg]
K_f : Freundlich constant relating the sorption capacity
1/n : empirical parameter relating the sorption intensity

β_1 : activity coefficient related to sorption mean energy [mol^2/KJ^2]
ϵ : polanyi potential
R : gas constant [8.314×10^{-3} kJ/molK]
T : temperature (Kelvin)
E : mean free energy of sorption per molecule of sorbate
B : heat of sorption
t : time [min]
K_T : equilibrium binding constant [L/mg]
a_s, K_s, β_s : sips parameter
b_T, n_T : toth parameter
K_1 : rate constant for the pseudo first order equation [min^{-1}]
K_2 : rate constant for the pseudo second order equation [g/mg min]
K_{id} : intra particle diffusion rate constant [mg/g $min^{-0.5}$]
K, v : power function constant
α : initial adsorption rate [mg/ g min]
β : desorption constant [g/mg]
K_R : separation factor (dimensionless)
K_a : isotherm constant

REFERENCES

1. P. Suksabye, P. Thiravetyan and W. Nakbanpote, *J. Hazard. Mater.*, **160**, 56 (2008).
2. C. Quintelas, B. Fonseca, B. Silva, H. Figueiredo and T. Tavares, *Bioresour. Technol.*, **100**, 220 (2009).
3. IARC, *Monographs on the evaluation of carcinogenic risks to humans: Overall evaluation of carcinogenicity,* An updating of IARC Monographs., France (1987).
4. M. Cieslak-Golonka, *Polyhedron*, **15**, 3667 (1995).
5. R. D. Baral, Engelken, *Environ. Sci. Pollut.*, **5**, 121 (2002).
6. B. Volesky, *Removal and recovery of heavy metals by biosorption, in: B. Volesky (Ed.), Biosorption of Heavy Metals*, CRC Press, Inc., Boca Raton, FL, USA (1990).
7. G. A. Zinkus, W. D. Byers and W. W. Doerr, *Chem. Eng. Prog.*, **94**(5), 19 (1998).
8. E. Harry, *Trends Biotechnol.*, **17**, 462 (1999).
9. P. Miretzky, A. Saralegui and A. FernandezCirelli, *Chemosphere*, **62**, 247 (2006).
10. B. Volesky, *Sorption and Biosorption*, BV-Sorbex Inc., Quebec, Canada (2003).
11. B. Volesky and Z. R. Holan, *Biotechnol. Prog.*, **11**, 235 (1995).
12. T. A. Davis, B. Volesky and R. H. S. F. Vieira, *Water Res.*, **34**, 4270 (2000).
13. P. Donghee, Y. Yeoung-Sang, A. ChiKyu and P. Jong Moon, *Chemosphere*, **66**, 939 (2007).
14. M. M. Areco, E. Valdman and M. D. S. Afonso, *J. Chem. Educ.*, **84**, 302 (2007).
15. G. J. Ramelow, D. Fralick and Y. Zhao, *Microbios.*, **72**, 81 (1992).
16. D. Roy, P. N. Greenlaw and B. S. Shane, *J. Environ. Sci. Health-Part A. Environ. Sci. Eng.*, **28**, 37 (1993).
17. Z. R. Holan, B. Volesky, *Biotechnol. Bioeng.*, **43**, 1001 (1994).
18. A. B. Ariff, M. Mel, M. A. Hasan and M. I. A. Karim, *J. Microbiol. Biotechnol.*, **15**, 291 (1999).
19. A. Van der Wal, W. Norde, J. B. Zhnder and J. Lyklema, *Colloids Surf., B*, **9**, 81 (1997).
20. A. Esposito, F. Paganelli and F. Veglio, *Chem. Eng. Sci.*, **57**, 307 (2002).
21. Z. R. Holan, B. Volesky and I. Prasetyo, *Biotechnol. Bioeng.*, **41**, 819 (1993).
22. K. H. Chong and B. Volesky, *Biotechnol. Bioeng.*, **47**, 451 (1995).
23. J. T. Matheickal and Q. Yu, *Bioresour. Technol.*, **69**, 223 (1999).
24. J. T. Matheickal, Q. Yu and G. M. Woodburn, *Water Res.*, **33**, 335 (1999).
25. A. Leusch, Z. R. Holan and B. Volesky, *J. Chem. Technol. Biotechnol.*, **62**, 279 (1995).
26. E. G. V. Percival and R. H. McDowell, *Chemistry and Enzymology of Marine Algal Polysaccharides*, London, UK: Academic Press (1967).
27. E. Fourest and B. Volesky, *Environ. Sci. Technol.*, **30**(1), 277 (1996).
28. T. A. Davis, B. Volesky and A. Mucci, *Water Res.*, **37**, 4311 (2003).
29. A. D. Eaton, L. S. Clesceri and A. E. Greenberg, *Standard methods for the examination of water and wastewater*, American Public Health association (APHA), AWWA, WPCF, Washington, DC (1995).
30. B. Volesky, *Hydrometallurgy*, **59**, 203 (2001).
31. M. Rajasimman and K. Murugaiyan, Seaweed Research and Utilization, **33**(1&2), 99 (2011).
32. A. Esposito, F. Pagnanelli and F. Veglio, *Chem. Eng. Sci.*, **57**(3), 307 (2002).
33. J. T. Matheickal and Q. Yu, *Bioresour. Technol.*, **69**(3), 223 (1999).
34. C. L. Rollinson, *Chromium, molybdenum and tungsten*, In: Trotman-Dickenson (Ed.), Comprehensive Inorganic Chemistry, third Ed. Pergamon Press, Oxford, 691 (1973).
35. S. R. Bai and T. E. Abraham, *Bioresour. Technol.*, **79**, 73 (2001).
36. S. Mor, R. Khaiwal and N. R. Bishnoi, *Bioresour. Technol.*, **8**, 954 (2006).
37. H. Barrera, F. Urena-Nunez, B. Bilyeu and C. Barrera-Diaz, *J. Hazard. Mater.*, **136**(3), 846 (2006).
38. Y. N. Mata, M. L. Blazquez, A. Ballester, F. Gonzalez and J. A. Munoz, *J. Hazard. Mater.*, **158**, 316 (2008).
39. A. V. Ajay Kumar, N. A. Darwish and N. Hilal, *World Appl. Sci.*, **5**, 32 (2009).
40. N. M. Salem and A. M. Awwad, *J. Saudi Chem. Soc.*, **18**(5), 379 (2014).
41. M. M. Areco and M. Dos Santos Afonso, *Colloid Surf., B: Biointerfaces*, **81**, 620 (2010).
42. R. Jalali, H. Ghafourian, Y. Asef, S. J. Davarpanah and S. Sepehr, *J. Hazard. Mater.*, **92**, 253 (2002).
43. P. Xin Sheng, Y. P. Ting, J. P. Chen and L. Hong, *J. Colloid Interface Sci.*, **275**, 131 (2004).
44. A. K. Meena, G. K. Mishra, P. K. Rai, C. Rajagopal and P. N. Nagar, *J. Hazard. Mater.*, **122**, 161 (2005).
45. Z. Chen, W. Ma and M. Han, *J. Hazard. Mater.*, **155**, 327 (2008).
46. M. Riaz, R. Nadeem, M. A. Hanif, T. M. Ansari and K. U. Rehman, *J. Hazard. Mater.*, **161**, 88 (2009).
47. N. Nasuha, B. H. Hameed and A. T. Mohd Din, *J. Hazard. Mater.*, **175**, 126 (2010).
48. G. Donmez and Z. Aksu, *Process Biochem.*, **38**(5), 751 (2002).
49. I. Langmuir, *J. Am. Chem. Soc.*, **40**, 1361 (1916).
50. C. P. Huang, E. H. Smith and W. J. Copper (Ed.), *Chemistry in Water Reuse*, Ann Arbor Science Publishers Inc., Michigan, 355 (1981).
51. E. S. Cossich, C. R. G. Tavares and T. M. K. Ravagnani, *Biomass.*

Electron. J. Biotechnol., **5**(2), 133 (2002).
52. A. Saravanan, V. Brindha, R. Manimekalai and S. Krishnan, *Indian J. Sci. Technol*., **2**, 53 (2009).
53. L. K. Cabatingan, R. C. Agapay, J. L. L. Rakels, M. Ottens and L. A. M. Van der Wielen, *Ind. Eng. Chem. Res.*, **40**, 2302 (2001).
54. S. Basha, Z. V. P. Murthy and B. Jha, *Chem. Eng. J.*, **137**, 480 (2008).
55. R. Aravindhan, B. Madhan, J. R. Rao and B. U. Nair, *J. Chem. Technol. Biotechnol*., **79**, 1251 (2004).
56. M. Y. Arica, I. Tuzun, E. Yalcin, O. Ince and G. Bayramoglu, *Process Biochem*., **40**, 2351 (2005).
57. V. Murphy, H. Hughes and P. McLoughlin, *Chemosphere*, **70**, 1128 (2008).
58. M. X. Loukidou, A. I. Zouboulis, T. D. Karapantsios and K. A. Matis, *Colloids Surf., A*, **242**, 93 (2004).
59. G. C. Donmez, Z. Aksu, A. Ozturk and T. Kutsal, *Process Biochem.*, **34**, 885 (1999).
60. V. K. Gupta, A. K. Shrivastava and N. Jain, *Water Res*., **35**, 4079 (2001).
61. D. Park, Y. S. Yun, C. K. Ahn and J. M. Park, *Chemosphere*, **66**, 939 (2007).
62. A. Sarl and M. Tuzen, *J. Hazard Mater.*, **160**, 349 (2008).
63. M. G. A.Vieira, R. M. Oisiovici, M. L. Gimenes and M. G. C. Silva, *Bio. Res. Tech.*, **99**, 3094 (2008).
64. L. Yang and J. P. Chen, *Bio. Res. Tech.*, **99**, 297 (2008).
65. X. S. Wang, Z. Li and C. Sun, *J. Hazard Mater.*, **153**, 1176 (2008).
66. S. V. Gokhale, K. K. Jyoti and S. S. Lele, *J. Hazard. Mater.*, **170**, 735 (2009).
67. L. Deng, Y. Zhang, J. Qin, X. Wang and X. Zhu, *Mine. Eng.*, **22**, 372 (2009).
68. A. V. Bankar, A. R. Kumar and S. S. Zinjarde, *J. Hazard. Mater.*, **170**, 487 (2009).
69. C. Bertagnolli, M. G. C. D. Silva and E. Guibal, *Chem. Eng. J.*, **237**, 362 (2014).
70. I. M. Dittert, H. D. L. Brandao, F. Pina, E. A. B. D. Silva, S. M. A. Guelli, U. D. Souza, A. A. U. D. Souza, C. M. S. Botelho, R. A. R. Boaventura and V. J. P. Vilar, *Chem. Eng. J.*, **237**, 443 (2014).
71. A. K. Bhattacharya, T. K. Naiya, S. N. Mandal and S. K. Das, *Chem. Eng. J.*, **137**, 529 (2008).
72. V. K. Gupta, M. Gupta and S. Sharma, *Water Res.*, **35**, 1125 (2001).
73. S. Arfaoui, N. Frini-Srasra and E. Srasra, *Desalination*, **222**, 474 (2008).
74. G. Arslan and E. Pehlivan, *Bioresour. Technol.*, **98**, 2836 (2007).
75. H. M. F. Freundlich, *J. Phys. Chem.,* **57**, 385 (1906).
76. M. M. Dubinin, *Chem. Rev.*, **60**, 235 (1960).
77. P. Lodeiro, J. L. Barriada, R. Herrero and M. E. Sastre de Vicente, *Environ. Pollut*., **142**, 264 (2006).
78. M. Sari and M. Tuzen, *J. Hazard. Mater*., **144**, 41 (2007).
79. M. J. Temkin and V. Pyzhev, Kinetics of ammonia synthesis on promoted Iron catalysts, ctaphysiochem URSS12, 217-256 (1940).
80. R. Apiratikul and P. Pavasant, *Bio. Res. Tech.*, **99**, 2766 (2008).
81. K. Vijayaraghavan, T. V. N. Padmesh, K. Palanivelu and M. Velan, *J. Hazard. Mater. B*., **133**, 304 (2006).
82. V. J. P. Poots, G. McKay and J. J. Healy, *J. Water. Pollut. Con. F.*, **50**, 926 (1978).
83. K. R. Hall, L. C. Eagleton, A. Acrivos and T. Vermeulen, *Ind. Eng. Chem. Fund*., **5**, 212 (1966).
84. S. Lagergren, About the theory of so-called adsorption of soluble substances, der Sogenannten adsorption gelosterstoffeKungliga Svenska Vetenskapsalka de Miens Handlingar., **24**, 1 (1898).
85. Y. S. Ho and G. McKay, *Process Biochem*., **34**, 451 (1999).
86. W. J. Weber and J. C. Morris, *J. Saint Eng. Div. Am. Soc. Civ. Eng.*, **89**, 31 (1963).
87. C. S. Sundaram, N. Viswanathan and S. Meenakshi, *Bioresour. Technol*., **99**, 8226 (2008).
88. Y. S. Ho, J. C. Y. Ng and G. McKay, *Sep. Purif. Rev*., **29**, 189 (2000).
89. S. Kuo and E. G. Lotse, *Soil. Sci. Soc. Am. Proc*., **38**, 50 (1974).
90. Y. Onal, *Hazard. Mater.*, **B137**, 1719 (2006).
91. H. Javadian, M. Ahmadi, M. Ghiasvand, S. Kahrizi and R. Katal, *J. Tai Inst. Chemi. Eng.*, **44**, 977 (2013).
92. M. Saeed and Iqbal, *Water Res.*, **37**, 3472 (2003).
93. D. Park, Y. S. Yun and J. M. Park, *Chemosphere*, **60**, 1356 (2005).
94. S. Tunali, I. Kiren and T. Akar, *Miner. Eng*., **18**, 681 (2005).
95. H. N. Bhatti, B. Mumtaz, M. A. Hanif and R. Nadeem, *Process Biochem*., **42**, 547 (2007).
96. Y. S. Yun, *J. Microbiol. Biotechnol*., **14**, 29 (2004).
97. R. Nadeem, T. M. Ansari and A. M. Khalid, *J. Hazard. Mater*., **156**, 64 (2008).
98. L. Ramrakhiani, R. Majumder and S. Khowala, *Chem. Eng. J*., **171**, 1060 (2011).
99. R. Saravanane, T. Sundararajan and S. Sivamurthyreddy, *Indian J. Environ. Health*, **44**, 78 (2002).
100. S. K. Mehta, B. N. Tripathi and J. P. Gaur, *J. Appl. Phycol*., **14**, 267 (2002).
101. S. Kalyani, P. S. Rao and A. Krishnaiah, *Chemosphere*, **57**, 1225 (2004).
102. A. Singh, D. Kumar and J. P. Gaur, *Bioresour. Technol*., **98**, 3622 (2007).
103. A. Singh, D. Kumar and J. P. Gaur, *J. Hazard. Mater*., **152**, 1011 (2008).
104. W. E. Marshall and E. T. Champagne, *J. Environ. Sci. Health*, **30**, 241 (1995).
105. T. R. Banga and S. G. Sharma, *Industrial organization and engineering economics*, 21st Ed., Khanna Publishers (1996).